Two-dimensional spin-1/2 rectangular Heisenberg antiferromagnets: Simulation and experiment

B. C. Keith, C. P. Landee, T. Valleau, M. M. Turnbull, and N. Harrison

Phys. Rev. B **84**, 104442 — Published 26 September 2011

DOI: 10.1103/PhysRevB.84.104442

Two-dimensional S=1/2 rectangular Heisenberg antiferromagnets: simulation and experiment

B. C. Keith, C. P. Landee, and T. Valleau
Department of Physics, Clark University, Worcester, MA, 01610

M. M. Turnbull
Carlson School of Chemistry and Biochemistry, Clark University, Worcester, MA, 01610

N. Harrison
National High Magnetic Field Laboratory, LANL, Los Alamos, New Mexico, 87545
(Dated: August 4, 2011)

We have simulated and analyzed the susceptibility of a series of two-dimensional S=1/2 rectangular Heisenberg antiferromagnetic (as well as mixed exchange antiferromagnetic/ferromagnetic) lattices as a function of J, J' and temperature, where J is the dominant magnetic exchange interaction and J', the orthogonal interaction, is related to J by $J' = \alpha\ J$, where α can vary from 0 to 1. Previous studies of the compounds pyrazineformatocopper(II) nitrate $[Cu(pz)(HCO_2)](NO_3)$, catena-2-aminopyrimidinedichlorocopper(II) $[Cu(2{-}apm)Cl_2]$, and catena-pyrazinediazidocopper(II) $[Cu(pz)(N_3)_2]$ indicated that these systems had two-dimensional magnetic spin-spin interactions. However, there were no two-dimensional models that could capture the behavior of any measurable bulk properties of the compounds. The previous authors fit the susceptibility data of the respective compounds to a one-dimensional antiferromagnetic chain with a mean field correction, or did not fit the data at all. We use the simulations to create this fit function in order to test the two-dimensional model proposed for these spin systems.

I. INTRODUCTION

An $S = 1/2$ quantum Heisenberg antiferromagnetic (QHAF) rectangular lattice may be characterized by a lattice of spin-1/2 particles which interact with each other via two orthogonal exchange pathways. One pathway is mediated by a magnetic exchange strength J while for the other pathway, strength J'. J is the dominant exchange and α, the aspect ratio, relates J and J' by $J' = \alpha J$, where α ranges from $0 \leq \alpha \leq 1$. The one-dimensional (1D) antiferromagnetic (AF) chain and the two-dimensional (2D) antiferromagnetic square magnetic lattice correspond to $\alpha = 0$ and 1, respectively. The Hamiltonian for such systems may be written

$$\vec{H} = J \sum_i [\vec{S}_i \cdot \vec{S}_{i+x} + \alpha \vec{S}_i \cdot \vec{S}_{i+x'}], \qquad (1)$$

where $\vec{S}_{i+x}$ ($\vec{S}_{i+x'}$) denotes a spin located adjacently to a spin S_i in the direction of J (J'). A negative J value indicates a ferromagnetic interaction as aligned spins would correspond to a lower energy state.

Theoretical interest in rectangular magnets can be traced back to the Haldane conjecture over 25 years ago.[1] Haldane showed that isolated integer-spin chains have a gap in their excitation spectrum at T=0 and thus do not exhibit long range order (LRO). Since then it has been shown that a finite coupling ($\alpha \sim 10^{-3}$) between integer spin chains will lead to LRO through Schwinger-Boson techniques[2] and through spin-wave theory.[3] The same question has been asked of half-integer spin chains, most notably the S=1/2 spin chain. Does Néel order set in for infinitesimal intrachain coupling or is there a finite α_c where the order-disorder tranisition takes place? Some mean field theories[2,3] indicate that a spin-1/2 chain will order at any infinitesimal coupling while spin-wave expansions and Lanczos techniques[4,5] have indicated that $\alpha_c < 0.1$.

Several compounds that display structural characteristics of a 2D rectangle have been studied; pyrazineformatocopper(II) nitrate $[Cu(pz)(HCO_2)](NO_3)^6$, catena-2-aminopyrimidinedichlorocopper(II) $[\mathrm{Cu}(2{-}apm)Cl_2]^7$, and catena-pyrazinediazidocopper(II) $[Cu(pz)(N_3)_2]^8$, where 2-apm=2-aminopyrimidine and pz = pyrazine. However, at the time of these original publications, there were no 2D rectangular QHAF models that related any of the measurable bulk properties of the system to J or J'. Instead, the susceptibilities of these compounds were fit to the model susceptibility of a 1D chain with a mean field correction or not at all. Since the 1D chain and a 2D QHAF produce similarly-shaped susceptibility curves, a reasonable fit was achieved with skewed parameters, most notably J and α.

The susceptibility of a 2D QHAF has not been solved analytically for any α greater than 0. However, there has been a great deal of study on the 2D square QHAF through monte carlo simulation techniques for both the isotropic[9,10] and anisotropic cases[11,12]. The susceptibilities of a family of 2D rectangular QHAF have been simulated and shown to successfully model data[13] with the help of the ALPS software[14]. We have expounded on this work by simulating the susceptibility curves of these systems for several different α values with a finer resolution and reformulating the curves into a fit function for general α. We endeavor to show that the aforementioned

compounds can be modeled as 2D QHAF's above their respective Néel ordering temperatures with exchange energies that are consistent with other compounds belonging to the same family.

We also present high field magnetization data for known rectangles pyrazinedichlorocopper(II) $[Cu(pz)Cl_2]$[15] and $[Cu(pz)(N_3)_2]$, providing further evidence for their rectangular 2D nature.

II. EXPERIMENTAL

A. Synthesis and characterization

Each compound was prepared according to the respective syntheses given in the original papers[6–8,15]. IR(infrared spectroscopy) spectra were recorded on a PE Paragon 500 spectrophotometer while powder XRD(x-ray diffraction) data were collected on a Bruker AXS D8 Focus X-ray diffractometer at angles of 5° up to 54.5° at room temperature. The purity of each compound was confirmed by comparing the XRD data to the published structures. IR spectra are consistent with this result.

B. Magnetic Measurements

Magnetic data were collected using a Quantum Design MPMS-XL SQUID magnetometer. Crystals were powdered and packed into a #3 gelatin capsule. The magnetization of the sample as a function of field was collected from 0 to 5 T at 1.8 K. Susceptibility data were taken over the temperature range from 1.8 to 300 K in an applied field of 1000 Oersteds.

High pulsed field magnetization data were taken for $Cu(pz)Cl_2$ at the National High Magnetic Field Lab (NHMFL) at Los Alamos National Labs (LANL) using a 65 Tesla short pulse magnet at temperatures between 0.4 and 4.0 K.

High field magnetization data was taken for $Cu(pz)(N_3)_2$ at the NHMFL at Florida using a 35 Tesla Bitter magnet at a temperature of 1.3 K.

C. Simulations

Simulated reduced magnetic susceptibility ($\chi^* = \chi J/C$) data for a series of antiferromagnetic rectangular magnetic lattices were generated as a function of reduced temperature T/J by means of quantum monte carlo simulations using the SSE looper code application of the ALPS libraries.[14] Simulations of the susceptibility for $\alpha = 0.5$ employed square lattices with L^2 number of spins, where $L = 8, 16, 32, 64$ were studied (Fig. 1). For the $L = 8$ and $L = 16$ lattices, the susceptibility approaches 0 at low temperature, indicative of a gap. This can not be correct in the gapless rectangular model; there must be too few spins to capture the properties of a 2D system. Small deviations in the $L = 32$ and $L = 64$ susceptibilities at $T/J = 0.02$ suggests that 4096 spins is sufficient to simulating the rectangular system, at least above $T/J = 0.02$ which is sufficiently low enough to compare to real systems within the limit of experimental temperatures. Simulations on $L > 64$ lattices take a prohibitively long time on our processors. Data were generated for temperatures in the range $0.01 - 2\ T/J$ in increments of $0.01\ T/J$, $2 - 10\ T/J$ in increments of $0.25\ T/J$, and $10 - 25\ T/J$ in increments of T/J for α 0 to 1 in 0.05 increments.

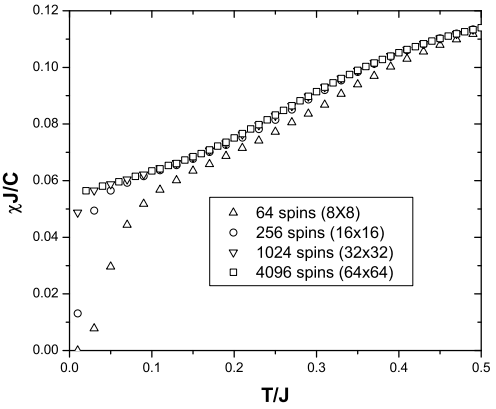

FIG. 1. Dimensionless susceptibilty of antiferromagnetic rectangles as a function of reduced temperature for $\alpha = 0.50$ and of increasing numbers of spins.

The simulated susceptibility in the limiting case of $\alpha = 0$ reaches a maximum value of $\chi_{max}J/C = 0.587644 \pm .000001$ at $T_{max}/J = 0.64 \pm .02$, where C is the Curie constant. This is consistent with the previously calculated value[16] of $\chi_{max}J/C \sim 0.58770511(6)$ at $T_{max}/J = .6408510(4)$ for the 1D antiferromagnetic chain. We can also fit the simulated curves to the known susceptibilities in the 1D and 2D square case as a further check of accuracy. Figure 2 shows the simulated 1D chain and 2D square susceptibilities. The susceptibility for the 2D square is consistent with previously reported simulated data[9,10] as it uses the same methods. The known 1D[17] and 2D[18] susceptibilities are fits to the simulated curves with errors less than 1 part in 10^5 in each case.

It is possible that α can take on negative values. In this case the rectangular magnetic lattice is said to be mixed exchange; If J is antiferromagnetic, then J' is ferromagnetic (FM). This will be referred to as an AF/fm lattice, the stronger exchange is capitalized. In this regime, the 1D antiferromagnetic chain and the isotropically mixed exchange AF/FM lattice correspond to $\alpha = 0$ and -1, respectively. If J is ferromagnetic and J' is antiferromagnetic then the lattice is labeled FM/af. In this alternate regime, the 1D ferromagnetic chain and the isotropically mixed exchange FM/AF magnetic lattice correspond to

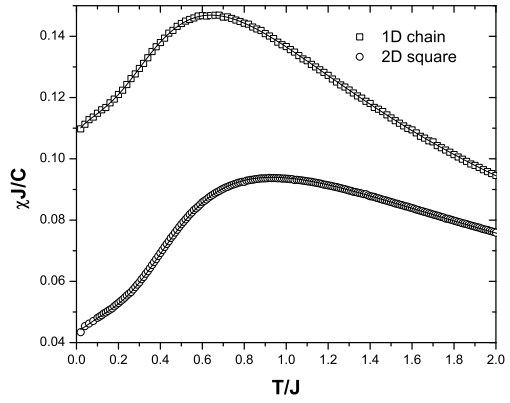

FIG. 2. The simulated susceptibilities of the 1D($\alpha = 0$) and 2D($\alpha = 1$) limits for the antiferromagnetic rectangles. Previously reported susceptibilities are shown as solid lines. There is no difference within the error bewteen the simulations and the known susceptibilities.

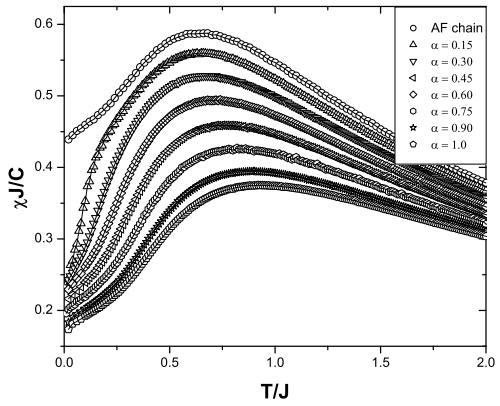

FIG. 3. Dimensionless susceptibilty of AF/af magnetic rectangles as a function of reduced temperature for several values of α. The bottom curve is the 2D square. Curves lie on top of the square lattice sequentially in order of decreasing α all the way to the 1D antiferromagnetic chain which is the topmost curve in increments of roughly 0.15. The numerically calculated coefficients from table I are shown as lines over the respective susceptibility curves.

$\alpha = 0$ and -1, respectively. Note that the isotropically mixed exchange AF/FM and FM/AF lattices are equivalent. Simulations for the AF/fm lattices and the FM/af lattices were also run with identical parameters to those mentioned for the antiferromagnetic lattices.

III. RESULTS AND DISCUSSION

A. Simulations

The susceptibilities as a function of reduced temperature for the AF/af lattices (Fig. 3) at different alpha values show rounded maxima before descending to finite values at low temperature, as expected for gapless systems. The temperatures at which these maxima occur increase systematically as alpha increases while the heights of the maxima decrease. The T=0 values that each curve approaches decreases as alpha increases.

The susceptibilities as a function of reduced temperature for AF/fm lattices (Fig. 4) also show rounded maxima before converging to finite values at low temperature. The temperature of these maxima as well as the values of the maxima increases systematically as alpha increases due to the introduction of increasingly strong ferromagnetic interactions. At low temperatures the curves cross each other and head towards finite susceptibilities with no clear pattern in values of α. The low temperature finite susceptibility values as well as the values for the maximum susceptibility are greater than in the AF/af case (Fig. 5) for the same values of $|\alpha|$.

The susceptibilities as a function of reduced temperature for FM/af lattices (Fig. 6) show rounded maxima before approaching finite values at low temperatures. The topmost curve, the isolated ferromagnetic

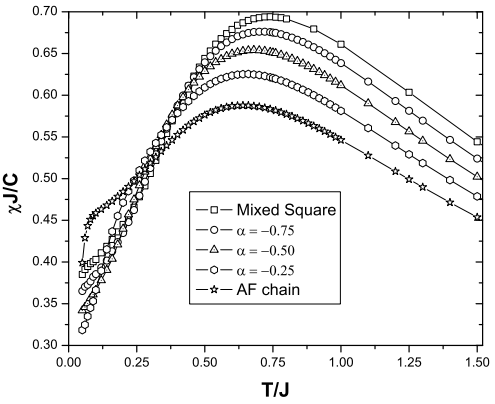

FIG. 4. Dimensionless susceptibilty of AF/fm magnetic rectangles as a function of reduced temperature for several values of α. The botttom curve is the isolated antiferromagnetic chain while the top curve is the isotropic AF/FM lattice. Lines have been drawn through the data as a guide to the eye.

chain which diverges at low temperature, is added for comparison. The temperature of these maxima as well as the value of the maximum susceptilities decrease in magnitude as alpha increases. The susceptibilities are suppressed overall as alpha increases for any given temperature.

It is easy to characterize a FM/af compound because one can find two unique and characteristic maxima from

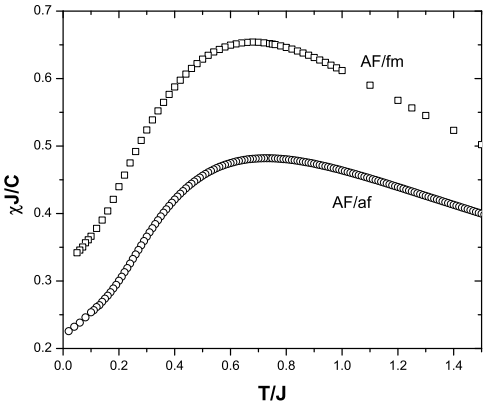

FIG. 5. Dimensionless susceptibility vs reduced temperature for AF/fm and AF/af rectangles of with $|\alpha| = 0.5$. The susceptibility is always greater for the AF/fm case for same $|\alpha|$.

bulk magnetic properties. Since the temperature of the maximum χ value, $T_{max}(\chi)$, and the temperature of the maximum χT value, $T_{max}(\chi T)$, are not proportional to each other we can use the ratio of the two maxima to determine the relative exchange strengths of the two exchanges. Plotting the unitless ratio $\frac{T_{max}(\chi)}{T_{max}(\chi T)}$ vs α reveals linear behavior over the whole range of $\alpha > 0$ described by the equation $\frac{T_{max}(\chi)}{T_{max}(\chi T)} \simeq -0.43\alpha + 0.42$(Figure 7).

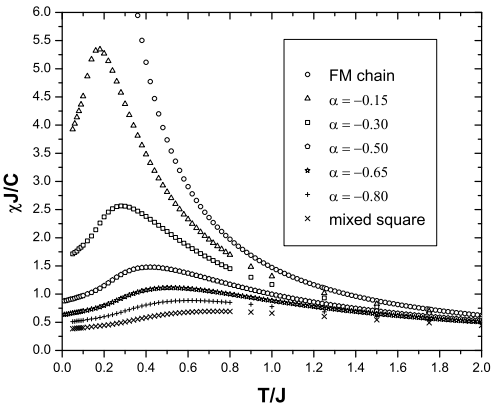

FIG. 6. Dimensionless susceptibilty of FM/af magnetic rectangles as a function of reduced temperature for several values of α. The topmost curve is the isolated ferromagnetic chain while the bottom curve is the isotropic AF/FM lattice. Notice the large difference in magnitude of this vertical scale compared to those of Figures 3 and 4.

The trend seen in the susceptibilities of these systems is consistent with what one would expect. As antiferromagnetic interactions increase or ferromagnetic interactions

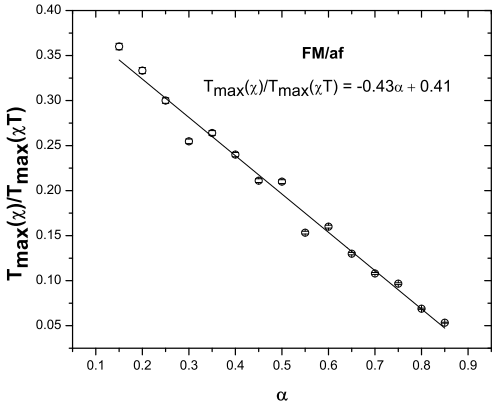

FIG. 7. The ratio of the temperatures of the maximum χ values and maximum χT values for the FM-af rectangles as a function of alpha. The ratio displays roughly linear behavior in the region between $0.15 < \alpha < 0.85$. This relationship provides a quick and easy estimate of the relative strengths of the interactions in a system.

are decreased, the value of the maximum susceptibility decreases. However, increasing the interaction strength in any way (antiferromagnetic or ferromagnetic) scales with the temperature of the maximum.

Fig. 8 is a plot of the normalized susceptibility temperature product (χ^*T/C) as a function of reduced temperature for representative values of $|\alpha|$ ranging from the isolated ferromagnetic chain to the isolated antiferromagnetic chain. In the regime where the antiferromagnetic interactions are stronger than the ferromagnetic interactions, χ^*T is always less than C. In the complementary regime, as temperatures increases, χ^*T always rises above the Curie constant and asymptotically settles back down to C at high temperatures (Fig. 9). When the antiferromagnetic strength equals the ferromagnetic strength, the χ^*T curve never exceeds C at any temperature. An experimental χ^*T curve with a maximum indicates dominant ferromagnetic interactions.

It would be useful to have a fit function that characterizes all of the simulated data. Such a function can be compared to experimental susceptibility data of a sample suspected of fitting the model of a Heisenberg rectangular magnetic lattice. From the quality of fit, we can extract the pertinent parameters; α, J, and C. We have formulated the fit function for the Heisenberg antiferromagnetic rectangular model using a modified Padé rational approximation to Curie's law in powers of J/T. The function for the reduced susceptibility (χ^*) as a function of α and temperature for an antiferromagnetic Heisenberg rectangular antiferromagnet is

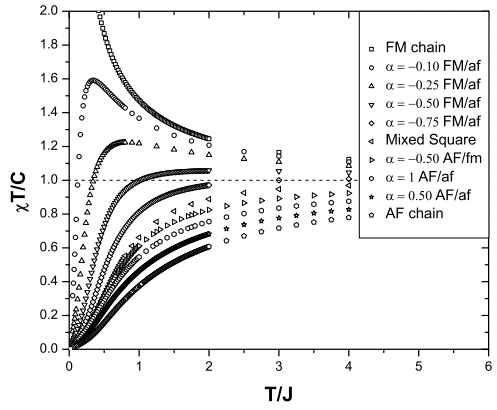

FIG. 8. Dimensionless susceptibility × temperature vs reduced temperature for Heisenberg magnetic rectangles of various α values. The isolated ferromagnetic chain is the topmost curve. As antiferromagnetic interactions are introduced the susceptibilities of the curves are supressed all the way to the isotropically mixed square AF/FM lattice. Each curve below the mixed square shows successively decreasing ferromagnetic interactions all the way down to no ferromagnetic interactions, the 1D antiferromagnetic chain.

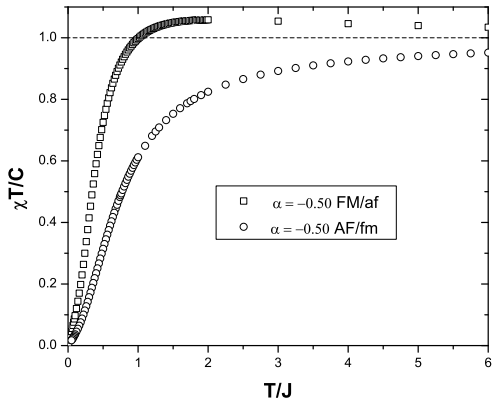

FIG. 9. Dimensionless susceptibility × temperature vs reduced temperature for Heisenberg magnetic rectangles of various α values. For strong ferromagnetic interactions, the χT data will always have a maximum and it will be greater than C.

$$\chi^*(\alpha,T) \equiv \frac{\chi(\alpha,T)J}{Ng^2\mu_\beta^2} = \frac{1}{4T}\frac{\sum_{n=0}^{6}[N_n(J/T)^n]}{\sum_{n=0}^{6}[D_n(J/T)^n]}, \quad (2)$$

where N is the number of spins, g is the gyromagnetic ratio, μ_β is the Bohr magneton and the coefficients are

$$\begin{aligned} N_0 &= D_0 = 1, \\ N_n(\alpha) &= \sum_{m=0}^{4} N_{nm}\alpha^m, \\ D_n(\alpha) &= \sum_{m=0}^{4} D_{nm}\alpha^m. \end{aligned} \quad (3)$$

We used this function to fit the surface of data provided by the whole set of simulation data taken for the AF/af rectangles. The fitting coefficients are given in table I. The solid lines in Fig. 3 were generated with this function.

The fit function also accurately fits the known extreme cases of the 1D antiferromagnetic chain ($\alpha = 0$) and the 2D uniform square lattice ($\alpha = 1$).

No equivalent fit function has been found that can characterize the simulated AF/fm or FM/af data.

Simulations of the magnetization as a function of applied field were also run using the ALPS dirloop code[14]. These simulations were compared to the high field magnetization data taken for $Cu(pz)Cl_2$ and $Cu(pz)(N_3)_2$ at temperatures of 0.4 K and 1.3 K respectively. Using the values of J found through susceptibility modeling, the simulations were run at a temperatures of $T/J = 0.016$ and a $T/J = 0.083$, respectively.

B. Rectangular systems

1. $Cu(pz)Cl_2$

The synthesis and structure for $Cu(pz)Cl_2$ have been previously reported.[15] $Cu(pz)Cl_2$ crystallizes (Fig. 10) in the monoclinic space group C2/m and contains planar centrosymmetric $Cu-X...Cu$ μ-bibridged chains along the c-axis that are linked together by $-Cu-pz-Cu-$ units along the b-axis, forming a rectangular structure. We have previously measured the susceptibility of this compound and modeled it as an AF/af rectangle of $\alpha =$ 0.30 with parameters[13] $J = 28$ K and Curie constant(C) = 0.426.

2. $Cu(pz)(N_3)_2$

The synthesis, structure and magnetic susceptibility for $Cu(pz)(N_3)_2$ has been previously reported[8]. $Cu(pz)(N_3)_2$ crystallizes (Fig. 11) in the monoclinic space group C2 and consists of chains of Cu-pz units connected by end-on azido bridges. The previous study[8]

parameters	$m=0$	$m=1$	$m=2$	$m=3$	$m=4$
N_{1m}	1519.2	533.43	-77.687	153.13	-169.91
N_{2m}	-215.7	100.15	124.18	-127.28	169.16
N_{3m}	218.14	-57.494	10.684	169.44	82.555
N_{4m}	-10.769	12.189	-227.21	45.305	-79.075
N_{5m}	0.094304	0.26961	27.093	128.89	-21.344
N_{6m}	-0.00089531	0.0093003	-0.17427	0.46488	0.38915
D_{1m}	369.44	126.42	13.757	-126.75	10.215
D_{2m}	179.27	254.16	234.59	69.668	-154.58
D_{3m}	50.271	106.25	-500.56	114.28	67.521
D_{4m}	95.893	-39.055	548.28	190.2	41.573
D_{5m}	-4.1906	13.921	-234.91	-242.49	-24.395
D_{6m}	-.00059343	-0.43284	27.795	117.38	43.919

TABLE I. Coefficients for equation 2, the AF/af rectangle fit function.

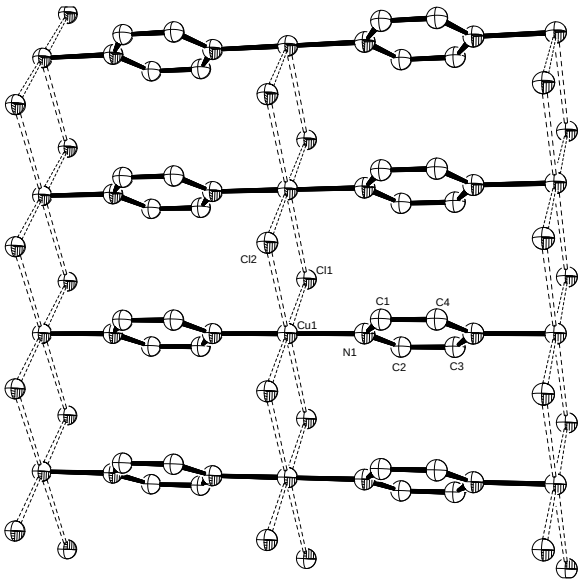

FIG. 10. Structure for $Cu(pz)Cl_2$. Chains of Cu-pz-Cu units are linked together through bibridged chlorides.

concluded that weak ferromagnetic interactions are mediated by the azido bridges while stronger antiferromagnetic interactions are mediated by the Cu-pz units.

3. $Cu(2-apm)Cl_2$

The synthesis and structure for $Cu(2-apm)Cl_2$ has been previously reported[7]. The crystal structure (Fig. 12) consists of 4+2 coordinate Cu^{2+} ions that are connected through two syn-anti 2-apm ligands as well as through bibridged chlorides through two short bonds and two long bonds. The authors[7] predicted that antiferromagnetic interactions should be mediated through both the 2-aminopyrimidine ligands and through the bibridged chlorides by analyzing the 2-apm/coordination plane dihedral angle but made no attempt to fit the susceptibility to a 2D QHAF model. It has been shown that the 3D

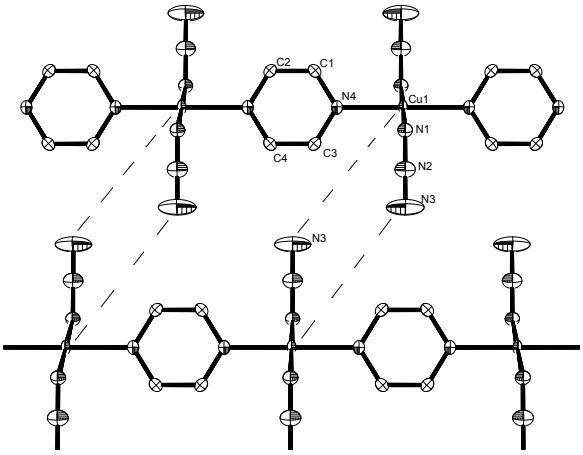

FIG. 11. Structure for $Cu(pz)(N_3)_2$. Cu-pz chains are connected through end-on azido bridges.

ordering temperature, T_n, of $Cu(pz)(N_3)_2$ is 2.8 K[19].

4. $[Cu(pz)(HCO_2)](NO_3)$

The synthesis and structure for $[Cu(pz)(HCO_2)](NO_3)$ has been previously reported[6]. $[Cu(pz)(HCO_2)](NO_3)$ crystallizes (Fig. 13) in the orthorhombic space group Pnma and consists of five-coordinate Cu^{2+} ions that are connected through syn-anti bridging μ-HCO_2^- and μ-pz ligands. The fifth coordination site is occupied by a terminal NO_3 group. Susceptibility data shows a maximum around 6.5K which indicates the presence of antiferromagnetic interactions. χT data also shows a maximum; as the sample is cooled the χT value rises before it falls rapidly towards 0 at low temperature. As discussed in Section III, this indicates a system with stronger ferromagnetic interactions and weaker antiferromagnetic interactions, the FM/af rectangle. The previous authors modeled the 2D spin lattice as an antiferromagnetic chain with a mean-field correction to account for interchain interactions. This apporach yielded an antiferromagnetic

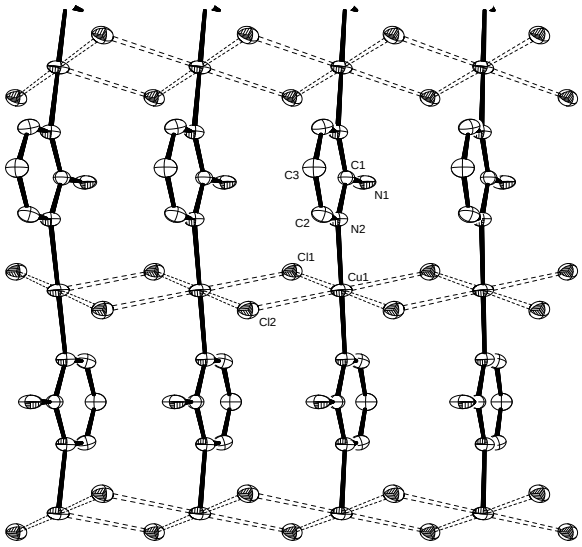

FIG. 12. Structure of one layer of $Cu(2-apm)Cl_2$. Chains are coupled together through bibridged chlorides.

intrachain coupling of J_{AFM} = -5.4 K and ferromagnetic interchain coupling of J_{FM} = 8.17 K.

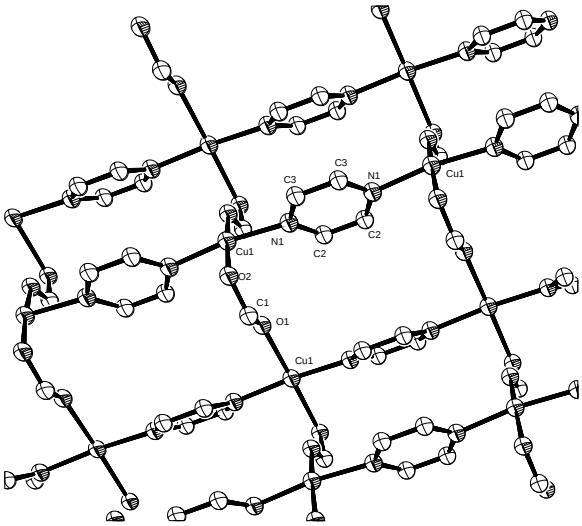

FIG. 13. Structure for $[Cu(pz)(HCO_2)](NO_3)$. It forms a 2D network of Cu^{2+} bridged by both pyrazine and $HCOO^-$ ligands. The terminal NO_3 groups(not shown) do not mediate any interactions and sit in the empty space between adjacent $HCOO^-$ and azide units.

C. Magnetic Data

1. $Cu(pz)Cl_2$

The magnetic behavior of $Cu(pz)Cl_2$ was initially reported by Hyde et al. who used the Ising linear chain model to model their data[20]. The magnetic behavior was reexamined by Inoue et al. using both susceptibility measurements and ^1HNMR measurements. Inoue et al. modeled the system as a Heisenberg linear chain with $J = 29.2K$[21]. The authors acknowledged that $Cu(pz)Cl_2$ mediates two orthogonal exchange pathways but that the lack of a 2D model prevented them from determining what the strength of the exchange is. They also note that the exchange strength through the bibridged chlorides must be significantly stronger than through the pyrazine bridges.

Subsequently, we[13] modeled the susceptibility data for $Cu(pz)Cl_2$ to the antiferromagnetic rectangle $\alpha = 0.30$ simulation that was discussed above with J = 28 K, αJ = 8.2 K, and Curie constant(C) = 0.426. $Cu(pz)Cl_2$ is known[22] to undergo antiferromagnetic 3D ordering at 3.2 K. The 2D rectangular simulations ignore 3D interactions and are not appropriate in the 3D limit so the data were fit from $7.5-325$ K which is a range of temperatures greater than twice the ordering temperature. The value of αJ = 8.2 K is identified as being mediated by the pyrazine bridges. This makes sense when we look back to a number of coordination compounds consisting of 2D layers of pyrazine that have been previously studied[23–25] by us as well as by others. The 2D square QHAF compounds $[Cu(pz)_2(2-pyridone)_2](ClO_4)$, $[Cu(pz)_2(ClO_4)_2]$, $[Cu(pz)_2(BF_4)_2]$, and $[Cu(pz)_2(NO_3)](PF_6)$ have in common that all the exchange interactions are mediated through pyrazine bridges only. The strengths of the exchanges range from $8-17.5$ K[24,25], which is consistent with αJ = 8.2 K for $Cu(pz)Cl_2$.

Now that the simulations have been combined into a model for susceptibility data for general α it is prudent to refit the $Cu(pz)Cl_2$ data to check for consistency. $Cu(pz)Cl_2$ was fit to the 2D AF/af rectangular model (Eq.2) (Fig 14a) with parameters $\alpha = 0.259 \pm .002$, $J = 28.46 \pm 0.05$ K, $\alpha J = 7.37 \pm 0.05$ K, $C = 0.418 \pm .001$ emu/mol $\cdot$ K, paramagnetic impurity $= 1.57\% \pm 0.02\%$ with a least square regression of $R^2 = 0.9999$. Again the fit was resolved over a temperature range of $7.5-325$ K to stay well above the 3D ordering temperature. These results are consistent with the previously reported result[13] and provides evidence that Eq. 2 is valid.

As a magnetic field is applied to a spin system, there is a torque on the spins that tends to make them align along the field direction. If this field is large enough, then it is possible to align all the spins, reaching a maximum net magnetization. This field is called the saturation field, or H_{SAT}. H_{SAT} has an associated magnetic energy commensurate to the sum of all the magnetic exchange energies in the lattice[26], as overcoming all the neighboring exchange strengths of each spin will allow all the spins to point freely in the direction of the field. For a rectangular system, every spin must gain enough energy to overcome two J components and two J' components and thus

$$g\mu_\beta H_{SAT} = (2J + 2J')k_B = 2J(1+\alpha)k_B. \qquad (4)$$

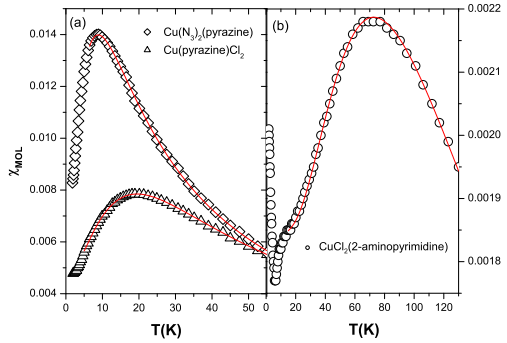

FIG. 14. (a): 2D QHAF model (Eq. 2) fits for $Cu(pz)(N_3)_2$ and $Cu(pz)Cl_2$ shown as curves superimposed with the data points. (b): 2D QHAF model (Eq. 2) fit for $Cu(2-apm)Cl_2$. The scale is an order of magnitude smaller than in (a) due to a very large antiferromagnetic interaction strength.

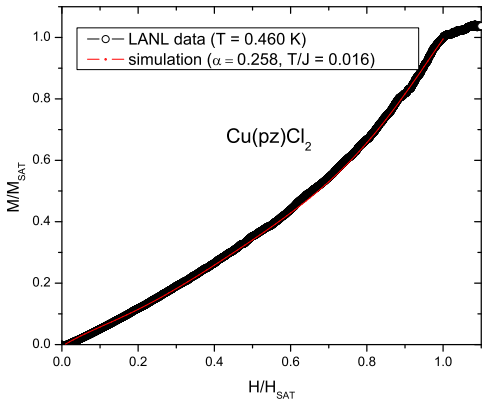

FIG. 15. High field pulsed magnetization data for $Cu(pz)Cl_2$. A simulation of the system is superimposed with the data.

where k_β is the Boltzmann's constant. This equation affords us an alternate way with which to determine the exchange strengths of an antiferromagnet.

High field magnetization data taken at $460mK$ for $Cu(pz)Cl_2$ (Figure 15, in units of the saturation field and magnetization) show a curve of steadily increasing slope up until a critical field where the slope of the curve dramatically flattens out. H_{SAT} is observed at 50.6 T. A Monte Carlo simulation is superimposed on the data at a $T/J = 460mK/28.46K = 0.016$ with $\alpha = 0.258$. The simulation undershoots the experimental curve from H/H_{SAT} of 0.3 up until about 0.9. We believe this discrepancy to be due to a significant background that can not be properly accounted for. More importantly, the simulated H_{SAT} meets the experimental H_{SAT} at an $H = 2.53J$, very close to the T=0 $H/J = 2.516$ calculated using equation 4. Plugging into equation 4 the values $\alpha = 0.258$, $J = 28.46$ K, as well as the previously reported[13] $g_{ave} = 2.128$, the T=0 $H_{SAT} = 50.2$ Tesla is estimated, in excellent agreement with the experimental value.

2. $Cu(pz)(N_3)_2$

The susceptibility data for $Cu(pz)(N_3)_2$ were previously fit[8] to an $S = 1/2$ 1D Heisenberg chain model with a mean field correction to account for the 2D interactions yielding an exchange energy J = 6.69 K and $J' =$ - 0.21 K. The authors[8] comment that for complexes with double end on azido bridging $\mu_{1,1}-N_3$, it has been proposed that for Cu-N-Cu angle values smaller than 105°, the coupling should be ferromagnetic[27]. Even though the angle is 99° for $Cu(pz)(N_3)_2$, an AF/fm model does not fit the data well at all. However, an AF/af rectangle model fits the susceptibility data very well (Fig. 14a). Since $T_n = 2.8$, the data was fit above $2T_n = 5.6K$ with parameters $\alpha = 0.46 \pm 0.01$, $\alpha J = 6.95 \pm .1$ K, $J = 15.1 \pm .1$ K, and $C = 0.431 \pm .001$ emu/mol with a least square regression of $R^2 = 0.99965$.

It was demonstrated[27] that the determination of the coupling through the $\mu_{1,1}-N_3$ bridge as ferromagnetic is not a hard and fast rule by citing that many compounds within this geometric range have J values (through the $\mu_{1,1}-N_3$ bridge) that range from -24 to 16.8 K. This still leaves the question of whether the stronger exchange is through the pyrazine bridge or the $\mu_{1,1}-N_3$ bridge. The values of $J = 15.1$ K and $\alpha J = 6.95$ K are both reasonable values for the exchange strength through either the $\mu_{1,1}-N_3$ bridge or the pyrazine bridge as shown earlier in this paper. Bulk magnetic measurements of the system are not enough to resolve this question though it seems plausible that the weaker exchange pathway (6.95 K) is through the $\mu_{1,1}-N_3$ bridge as the $Cu-N$ distance is quite long (2.001 $\AA$).

High field magnetization data for $Cu(pz)(N_3)_2$ at 1.3 K (figure 16) produce a curve of increasing slope up until around 26 Tesla where the curve starts to flatten out horizontally. At 32 Tesla the curve turns over and has almost reached magnetic saturation. The y-axis for the data was measured as a voltage, uncalibrated to emu/mol. This data was calibrated by comparison to 0-5 Tesla magnetization data taken on Clark University's SQUID magnetometer, where the y-axis is calibrated to emu/mol. At 32 Tesla the magnetization has a reading of 6280 emu/mol, corresponding to a g-factor of 2.26. The saturation value of a mol of spins with a g-factor of 2.14 (as is the case for this compound[8]) is 5975 emu/mol. We can not account for this curious discrepancy.

A Monte Carlo simulation is superimposed on the data at a T/J = 1.3 K/15.1K = 0.083 with $\alpha = 0.46$. The simulation was scaled up to the units of the experimental data for comparison as the experimental data could not be scaled down to dimensionless units due to the fact that

saturation was not reached. The parameters for the simulation are in excellent agreement with the data, giving two independent measures of the exchange parameters of the system.

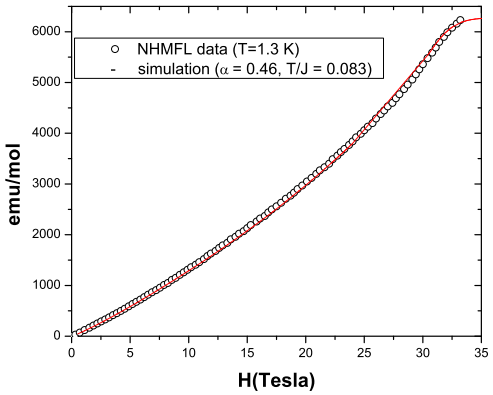

FIG. 16. High field magnetization data for $Cu(pz)(N_3)_2$. A simulation of the system with $\alpha = 0.46$, $J = 15.1$ K, $\alpha J = 6.9$ K, and $g_{ave} = 2.26$ is superimposed with the data.

The fact that magnetic saturation has not been reached by 32 Tesla shows that the previously reported values for the antiferromagnetic exchange interactions(6.69K and -0.21 K) can not be correct as these values estimate an $H_{SAT} = 10.1$ Tesla based on Eq. 4, clearly inconsistent with the data. We ignore the J' term in Eq. 4 as a ferromagnetic interaction would not influence the saturation field. Using our exchange parameters of $J = 15.1$ K and $\alpha J = 6.95$ K and Eq. 4 we calculate an $H_{SAT} = 32.3$ Tesla, consistent with our high field magnetization data.

3. $Cu(2-apm)Cl_2$

Figure 14b shows the susceptibility as a function of temperature for $Cu(2-apm)Cl_2$. The temperature of the maximum occurs at about 70 K while the value of the maximum is an order of magnitude smaller than in the cases of $Cu(pz)Cl_2$ and $Cu(pz)(N_3)_2$, indicating very strong antiferromagnetic interactions. The susceptibility data for $Cu(2-apm)Cl_2$ were fit (Fig. 14b) to a 2D QHAF rectangular model (Eq. 2) with parameters $\alpha = 0.084 \pm 0.002$, $J = 116.3 \pm 0.2$ K, $C = 0.448 \pm .001$ emu/mol, and paramagnetic impurity $= 2.85 \pm .05\%$ and a least squares regression of $R^2 = 0.99921$. A kink in the data can be seen near 10 K. It is likely that the material 3D orders near this temperature and thus the susceptibility was only modeled over the range 20-150 K.

There have been many studies[13,28,29] done on substituted-pyrazine compounds where bibridging chloride groups mediate antiferromagnetic exchanges between adjacent copper atoms. For the six compounds studied, the strengths of the antiferromagnetic exchanges through the bibridged chlorides range from 23.7-28 K. It is hard to believe that either the weaker($\alpha J = 9.7$ K) or stronger exchange($J = 116.3$ K) in $Cu(2-apm)Cl_2$ is mediated by the bibridged chlorides. To our knowledege, nothing in the literature refers to structures with bridging 2-apm ligands. At the moment, there is not enough information to even make a reasonable guess as to which pathway mediates the stronger exchange interaction.

4. $[Cu(pz)(HCO_2)](NO_3)$

Our susceptibility measurements of $[Cu(pz)(HCO_2)](NO_3)$ (Fig 17) show a maximum value of 0.0448 emu/mol at 6.5 K before asymptotically heading to the value of 0.036 emu/mol at 1.8 K, consistent with the published[6] maximum value of 0.0438 emu/mol at 6.6 K and low temperature value of 0.033 emu/mol at 2 K.

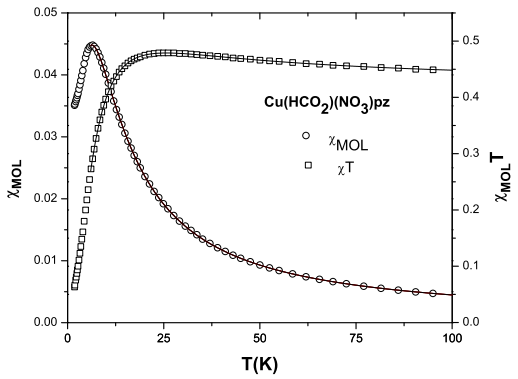

FIG. 17. Quantum Heisenberg FM/af model fit of both the χT and χ data for $[Cu(pz)(HCO_2)](NO_3)$. The maximum seen in the χT data indicates dominant ferromagnetic interactions.

The χT data reach a broad maximum near 26 K before heading towards zero at low temperatures. The susceptibility simulations for the FM/af rectangles are the only simulations to show a maximum in the χT data, therefore we fit the susceptibility to a FM/af model. For $Cu(pz)(HCO_2)(NO_3)$ the ratio of the temperatures of the maximums of χ and χT is $\frac{T_{max}(\chi)}{T_{max}(\chi T)} = \frac{6.5}{25.31} = 0.26$ and corresponds to $\alpha = -0.35$ by use of the fit in Figure 7. The ordering temperature has been shown to be $T_n = 3.66$ K[30] and thus the simulations are only valid above that temperature. Data were fit between 7.4 K and 150 K to ensure that the simulation didn't attempt to model any part of the 3D ordered phase. χT data were also modeled using the product of the simulated susceptibilities and reduced temperature. This technique affords us

a unique and alternate way to fit FM/af rectangles. The parameters yielded for both fits should be equal to each other.

This estimate of the relative exchange strengths (given above) of $\alpha = -0.35$ for $[Cu(pz)(HCO_2)](NO_3)$ is very good as the fitting parameters for χ and χT are extremely close to each other (see below and Table II). Attempts to fit the data at surrounding α values ($\alpha = -0.30, -0.40$) result in largely incommensurate fit parameters (Table II). Figure 17 shows the model fit for $[Cu(pz)(HCO_2)](NO_3)$ of an FM/af rectangle of $\alpha = -0.35$. χT data was fit with parameters $\alpha = -0.35 \pm 0.002$, $C = 0.426 \pm 0.001$ emu/mol, $J = -21.16 \pm 0.2$ K, paramagnetic impurity $= 5.16 \pm .05\%$ while χ data were fit with parameters $\alpha = -0.35 \pm 0.002$, $C = 0.424 \pm 0.001$ emu/mol, $J = -20.98 \pm 0.2$ K, paramagnetic impurity $= 3.81 \pm 0.05\%$, both in stark contrast to the previously reported values[6] of $J_{AF} = 5.4K$ and $J_{FM} = -8.17K$. This shows that the mean field approximation used[6] is innappropriate for this system.

The previous authors estimated the relative strengths of the two exchange pathways[30] by performing spin dimer analysis[31] on the basis of extended Huckel tight binding calculations[32]. The analysis showed that the HCO_2^- bridges mediate ferromagnetic interactions while the pyrazine bridges mediate antiferromagnetic interactions, consistent with the absence of any known ferromagnetic pyrazine bridge. Ferromagnetism has been observed[33] in compounds with bridging HCO_2^- units of certain configuration. Thus the HCO_2^- units mediate the ferromagnetic interactions while the pyrazine bridges mediate the antiferromagnetic interactions. The J value through the HCO_2^- bridge is $J = -21.2K$ while the J value through the pyrazine bridge is $J = 7.4$. The value of the exchange strength through the pyrazine bridge is consistent with the range of pyrazine exchange strengths (8-17.5 K) discussed in III.C.1 of this paper.

IV. CONCLUSIONS

We have investigated several 2D QHAF rectangular molecular magnets ($[Cu(2-apm)Cl_2]$, $[Cu(pz)(N_3)_2]$ and $[Cu(pz)Cl_2]$) through susceptibility and high field magnetization measurements. A 2D rectangular QHAF model has been found through a combination of simulations as well as theoretical techniques and is shown to be consistent with experiment. It has also been demonstrated that a real mixed exchange FM/af lattice exists ($[Cu(pz)(HCO_2)](NO_3)$) and that susceptibility simulations successfully model it.

V. AKNOWLEDGEMENTS

The authors thank the team responsible for the ALPS project, a library of simulations and algorithms for condensed matter monte carlo simulations. We used these simulations to model the magnetization and susceptibilities of our compounds. The Clark University Quantum Design MPMS-XL magnetometer was purchased with the assistance of the NSF and the Kresge Foundation. A portion of this work was performed at the National High Magnetic Field Laboratory (both at Talahassee and at Los Alamos National Lab) which is supported by NSF Cooperative Agreement No. DMR-9527035 and by the State of Florida.

	α = -0.30		α = -0.35		α = -0.40	
	χ	χT	χ	χT	χ	χT
C(emu · K/mol)	0.408	0.416	0.422	0.424	0.432	0.414
J(K)	-23.7	-24.81	-20.6	-20.9	-18.1	-16.1

TABLE II. χ and χT fitting parameters for $[Cu(pz)(HCO_2)](NO_3)$. The ratio of the temperatures of the maximums ($\frac{T_{max}(\chi)}{T_{max}(\chi T)}$) correspond to $\alpha = -0.35$. This estimate is on mark as the fitting parameters for χ and χT are extremely close to each other and the Curie constant is closest to the accepted value for copper of 0.42. Attempts to fit the data at surrounding α values ($\alpha = -0.30, -0.40$) result in inconsistent fit parameters as well as fit curves that miss key features of the data.

[1] F. Haldane, Phys Lett. 93A **463**, 1153 (1983).
[2] M. Azzouz and B. Doucot, Phys. Rev. B **47**, 8660 (1993).
[3] T. Sakai and M. Takahashi, J. Phys. Soc. Jpn. **58**, 3131 (1989).
[4] A. Parola, Phys. Rev. B **40**, 7109 (1989).
[5] A. Parola, S.Sorella, and Q. Zhong, Phys. Rev. Lett. **71**, 4393 (1993).
[6] J. Manson, T. Lancaster, J. Schleuter, S. Blundell, M. Brooks, F. Pratt, C. Nygren, H.-J. Koo, D. Dai, and M.-H. Whangbo, Inorganic Chemistry **46**, 213 (2007).
[7] B. J. Prince, M. M. Turnbull, and R. D. Willett, J. Coord. Chem. **56**, 441 (2003).
[8] W. Dong, Y. Ouyang, D.-Z. Liao, S.-P. Yan, P. Cheng, and Z.-H. Jiang, Inorganica Chimica Acta **359**, 3363 (2006).
[9] J.-K. Kim and M. Troyer, Phys. Rev. Lett. **80**, 2705 (1998).
[10] A. W. Sandvik, AIP Conf. Proc. **1297**, 135 (2010).
[11] J. Kim and R. J. Birgeneau, Phys. Rev. B. **62**, 6378 (2000).
[12] F.-J. Jiang, F. Kamper, and M. Nyfeler, Phys. Rev. B **80**, 033104 (2009).
[13] R. T. Butcher, C. P. Landee, M. M. Turnbull, and F. Xiao, Inorganica Chimica Acta **361**, 3654 (2008).
[14] F. Alet, P. Dayal, A. Grzesik, A. Honecker, M. Koerner, A. Laeuchli, S. R. Manmana, I. McCulloch, F. Michel, R. M. Noack, G. Schmid, U. Schollwoeck, F. Stoeckli, S. Todo, S. Trebst, M. Troyer, P. Werner, and S. Wessel, J. Phys. Soc. Jpn. Suppl. **70**, 30 (2005).
[15] J. Pickardt and B. Staub, Z. Naturforsch **52**, 1456 (1997).
[16] A. Klumper and D. C. Johnston, Phys. Rev. Lett. **84**, 4701 (2000).
[17] S. Eggert, I. Affleck, and M. Takahashi, Phys. Rev. Lett. **73**, 332 (1994).
[18] F. M. Woodward, A. S. Albrecht, C. M. Wynn, C. P. Landee, and M. M. Turnbull, Phys. Rev. B **65**, 144412 (2002).
[19] T. Valleau, Masters Thesis (unpublished).
[20] K. Hyde, G. Kokoszka, and G. Gordon, J. Inorg. Nucl. Chem. **31**, 1993 (1969).
[21] M. Inoue, S. Emori, K. Hara, and M. Kubo, J. Magn. Reson. **17**, 212 (1975).
[22] T. Lancaster, S. J. Blundell, F. L. Pratt, M. L. Brooks, J. L. Manson, E. K. Breechin, C. Cadiou, D. Low, E. J. L. McInnes, and R. E. P. Winpenny, J. Phys. C **16**, S4563 (2004).
[23] M. M. Turnbull, A. S. Albrecht, G. B. Jameson, and C. P. Landee, Mol. Cryst. Liq. Cryst. **335**, 245 (1999).
[24] V. Selmani, C. P. Landee, M. M. Turnbull, J. L. Wikaira, and F. Xiao, Inorg Chem Comm. **13**, 1399 (2010).
[25] F. Xiao, F. Woodward, C. Landee, M. Turnbull, C. Mielke, N. Harrison, T. Lancaster, S. Blundell, P. Baker, P. Babkevich, and F. L. Platt, Phys. Rev B **79**, 134412 (2009).
[26] L. J. Dejongh, W. D. V. Amstel, and A. R. Miedema, Advances in Physics **23**, 1 (1974).
[27] S. Triki, C. Garcia, E. Ruiz, and J. Pala, Inorg. Chem. **44**, 5501 (2005).
[28] K. Takeda, Y. Yamamoto, and T. Haseda, Phys. Lett A **45**, 419 (1973).
[29] S. N. Herringer, A. J. Longendyke, M. M. Turnbull, C. P. Landee, J. L. Wikaira, G. B. Jameson, and S. G. Telfer, Dalton Trans. **39**, 2785 (2010).
[30] J. L. Manson, J. G. Lecher, J. Gu, U. Geiser, J. A. Schlueter, R. Henning, X. Wang, A. J. Schultz, H.-J. Koo, and M.-H. Whangbo, Dalton Trans. **2003**, 2905 (2003).
[31] M.-H. Whangbo, H.-J. Koo, and D. J. Dai, Solid State Chem. **176**, 417 (2003).
[32] R. J. Hoffman, J. Chem. Phys. **39**, 1397 (1963).
[33] M. G. Alvarez, G. Alzuet, J. Borras, B. Marcias, and A. Castineiras, Inorg Chem **42**, 2992 (2003).